



Local and whole-body SAR in UHF body imaging: Implications for SAR matrix compression

Thomas M. Fiedler¹  | Mark E. Ladd^{1,2,3,4} | Stephan Orzada^{1,2} 

¹Medical Physics in Radiology, German Cancer Research Center (DKFZ), Heidelberg, Germany

²Erwin L. Hahn Institute for MRI, University Duisburg-Essen, Essen, Germany

³Faculty of Physics and Astronomy, Heidelberg University, Heidelberg, Germany

⁴Faculty of Medicine, Heidelberg University, Heidelberg, Germany

Correspondence

Thomas M. Fiedler, German Cancer Research Center (DKFZ), Division of Medical Physics in Radiology, Im Neuenheimer Feld 280, 69120 Heidelberg, Germany.
Email: t.fiedler@dkfz-heidelberg.de

Abstract

Purpose: Transmit arrays for body imaging have characteristics of both volume and local transmit coils. This study evaluates two specific absorption rate (SAR) aspects, local and whole-body SAR, of arrays for body imaging at 7 T and also for a 3 T birdcage.

Methods: Simulations were performed for six antenna arrays at 7 T and one 3 T birdcage. Local SAR matrices and the whole-body SAR matrix were computed and evaluated with random shims. A set of reduced local SAR matrices was determined by removing all matrices dominated by the whole-body SAR matrix.

Results: The results indicate that all RF transmit coils for body imaging in this study are constrained by the local SAR limit. The ratio between local and whole-body SAR is nevertheless smaller for arrays with large FOV, as these arrays also expose a larger part of the human body. By using the whole-body SAR matrix, the number of local SAR matrices can be reduced (e.g., 33.3% matrices remained for an 8-channel local array and 89.7% for a 30-channel remote array; 12.1% for the 3 T birdcage).

Conclusion: For transmit antenna arrays used for body imaging at 7 T as well as for the 3 T birdcage, all evaluated cases show that the local SAR limit was reached before reaching the whole-body SAR limit. Nevertheless, the whole-body SAR matrix can be used to reduce the number of local SAR matrices, which is important to reduce memory and computing time for a virtual observation points (VOP) compression. This step can be included as a pre-compression prior to a VOP compression.

KEYWORDS

local SAR, UHF body imaging, VOPs, whole-body SAR

1 | INTRODUCTION

Ultra-high-field (UHF) MRI uses multi-channel RF transmit antenna arrays and parallel transmit (pTx) techniques

to influence the B_1^+ distribution by the superposition of the antenna element fields with different amplitudes and phases. Not only the magnetic, but of course the

This is an open access article under the terms of the [Creative Commons Attribution-NonCommercial](https://creativecommons.org/licenses/by-nc/4.0/) License, which permits use, distribution and reproduction in any medium, provided the original work is properly cited and is not used for commercial purposes.

© 2024 The Author(s). *Magnetic Resonance in Medicine* published by Wiley Periodicals LLC on behalf of International Society for Magnetic Resonance in Medicine.

electric field varies with the time-dependent amplitudes and phases, leading to a different distribution of the specific absorption rate (SAR) for each set of complex weightings.¹ Thus, SAR is now a function of the complex excitation vector $u(t)$ containing all amplitudes and phases, and not simply a function of total input power as in single-channel transmit systems.² With a pre-calculated set of normalized SAR matrices $Q(r)$, representing the electric field contribution and dielectric tissue properties of the human body, SAR can be calculated using the quadratic form: $SAR(r, t) = \vec{u}^H(t) \cdot Q(r) \cdot \vec{u}(t)$.³ This separation of the spatial and temporal dependencies allows for the integration of SAR into pulse optimizations and RF safety supervision schemes.^{4,5}

The IEC guidelines define limits for local RF transmit coils and for volume RF transmit coils.⁶ Volume transmit coils shall be controlled with conservative estimates of whole-body SAR, head SAR, and at least one of the following: partial body SAR or local SAR. Local transmit coils shall be controlled by conservative estimates of local SAR and whole-body SAR. Local SAR is averaged over any 10 g of tissue in the body ('10 g-averaged' or local SAR). The IEC limits for the global and local SAR aspects for different operating modes are defined in the IEC guidelines⁶ and are reprinted in the supporting information (Table S1). According to the IEC, multi-channel transmit coils can have attributes of both local and volume RF transmit coils, and the appropriate control of SAR depends on the use of the coil. (In the previous edition 3.2 of the IEC guideline, volume transmit coils had to be controlled with conservative estimates of whole-body SAR and partial body SAR, including head SAR).

Local SAR cannot be measured in vivo during an MR examination and numerical simulations with realistic anatomical body models are required to achieve information on the field distribution within the body.^{1,7} Typically, a SAR matrix (size $N_c \times N_c$ where N_c is the number of transmit channels) for each 10 g-volume in the body is computed, resulting in a set of several million local SAR matrices for a whole-body model, which requires large amounts of memory and computational resources to determine the maximum local SAR for each RF pulse. Therefore, local SAR supervision is a major obstacle in the (real-time) safety supervision of pTx systems. To reduce the number of matrices, Eichfelder and Gebhard introduced the concept of virtual observation points (VOPs), where a compressed set of matrices is computed, reducing the number of matrices to be supervised from several million to a few hundred.⁸ However, the compression algorithm incorporates an overestimation factor, which is defined as a percentage of the worst-case SAR and leads to an overestimation in local SAR. In contrast, each global SAR

aspect can be expressed with a single matrix and no VOP compression is required.

RF transmit antenna arrays can be placed behind the boreliner and integrated into the MR system. This installation allows for a higher number of antenna elements and a larger FOV compared to classical local arrays placed close to the subject. These antenna arrays expose a large part of the human body, which raises questions regarding whole-body SAR.

This study evaluates local and whole-body SAR in various antenna arrays for body imaging at 7 T MRI. Such arrays have characteristics of both volume and local transmit coils, and it is common that both SAR aspects are considered during safety monitoring. For comparison, also a 3 T birdcage is assessed. Furthermore, the study evaluates the implications of the whole-body SAR aspect on the local SAR matrix compression.

2 | METHODS

Six 7 T antenna arrays were evaluated in this study, consisting of 25 cm-long microstrip antennas with meanders (Figure 1).^{9–12} The antenna elements were either placed close to the body (local arrays) or distant from the body and integrated into the MR system behind the bore liner (remote arrays). Remote arrays allow for a higher number of elements compared to local arrays due to the increased circumference, but typically expose a larger part of the human body. The elements can also be placed in multiple rings, increasing the FOV in the longitudinal direction, but also increasing the exposed body mass. In addition, a 2-channel birdcage for 3 T with 45 cm length was included.¹⁰ The simulation model includes the MR environment consisting of patient table and bore liner (595 mm inner diameter, 10 mm thickness, and $\epsilon'_r = 4.805$ and $\tan(\delta) = 0.0045$ at 297 MHz).¹⁰ The gradient shield (68 cm inner diameter, 122 cm long) and other metal parts were modeled as perfect electric conductors. Open boundaries were applied around the model.

A male body model (34 y, height 1.77 m, body mass 70.3 kg)¹³ was placed with the liver/kidney region in the center of each antenna model. All configurations were simulated with the arms placed to the left and right of the body. In addition, the 30-channel array was simulated with the arms above the head. EM field simulations were performed by using CST Studio Suite (Dassault Systèmes, Vélizy-Villacoublay, France). The electric field distributions and body tissue properties (conductivity and density) were exported to Matlab, and the local SAR matrices ($Q_{l,i}$) and the whole-body SAR matrix (Q_{wb}) were computed with

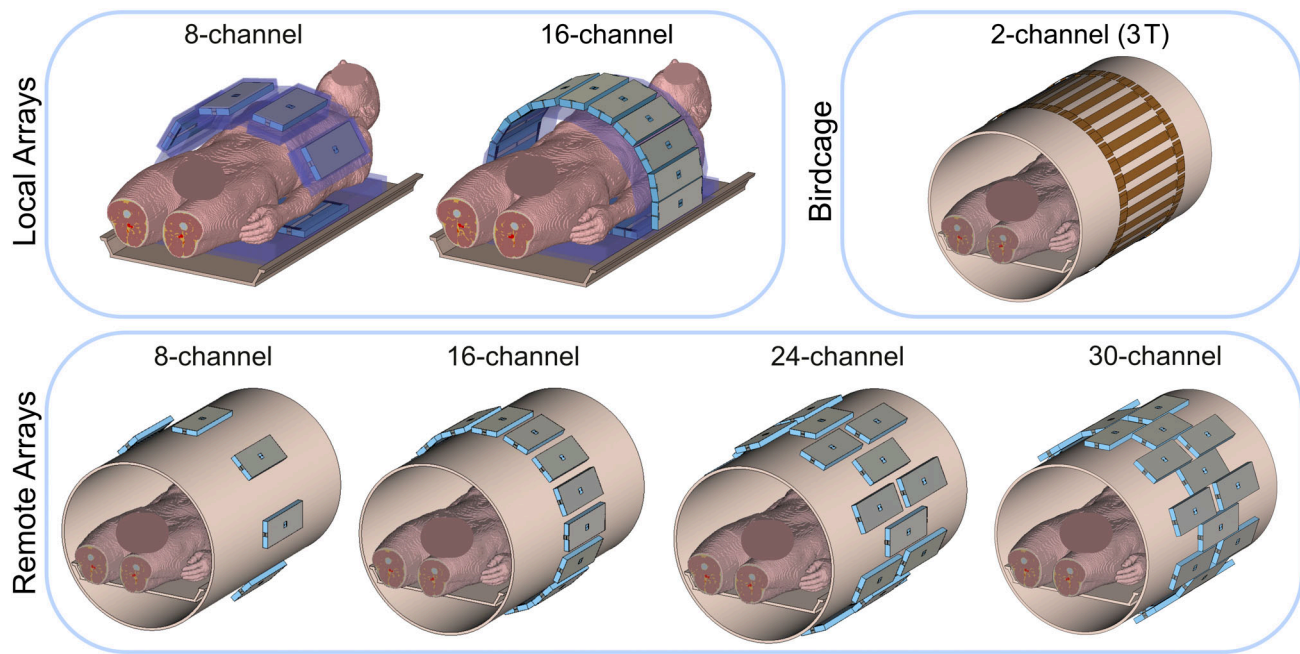


FIGURE 1 Local (8-channel, 16-channel) and remote (8-channel, 16-channel, 24-channel, 30-channel) 7 T antenna arrays consisting of 25 cm-long meander microstrip antennas. The remote arrays are placed outside the bore liner of the magnetic resonance patient tunnel. The 24- and 30-channel arrays consist of three interleaved rings with a 55 cm FOV in the longitudinal direction. The two-channel 3 T birdcage is 45 cm long.

an in-house toolbox:

$$Q(r) = \frac{1}{V} \int \frac{\sigma(r)}{2\rho(r)} \vec{E}^H(r) \cdot \vec{E}(r) dV$$

where E is the electric field vector normalized to the transmit signal $u(t)$ in unit V. The integration volume V is 10 g for the local SAR matrices and the body mass for the whole-body SAR matrix.¹⁴ With the complex transmit signal $u(t)$, SAR can be calculated for every time point:

$$\text{SAR}(r, t) = \frac{1}{T} t \Delta \int \vec{u}^H(t) \cdot Q(r) \cdot \vec{u}(t) dt.$$

To analyze which SAR limit is reached first, the ratio of local to whole-body SAR was calculated with 1 million random shims for the complex voltage of the transmit signal $u(t)$.

Local and whole-body SAR are restricted by different limits (cf. Table S1). For example, the local SAR limit is 10 W/kg and the whole-body SAR limit 2 W/kg in normal operating mode and for an averaging time of 6 min. Thus, a ratio of 5 in the evaluation of local vs. whole-body SAR corresponds to an equivalent restriction of both limits; values above 5 indicate a restriction by local SAR limits.

In this comparison, no VOP compression and therefore no overestimation was used in order to evaluate local SAR without overestimation. However, one configuration

was also calculated with VOPs to show the effect of different overestimations during the VOP compression on local SAR. For this purpose, the algorithm by Eichfelder and Gebhard was used with 2.5, 5 and 10% overestimation of worst-case SAR as well as the hybrid algorithm presented by Orzada et al. with 0.25 and 1% overestimation. Worst-case SAR, which is the highest SAR any combination of magnitudes and phases in the complex excitation vector can reach, is considered for the overestimation in an Eichfelder VOP compression⁸ and was determined by the maximum eigenvalue of all SAR matrices in the body for an eigenvector of unit voltage ($\|u\| = 1$). The ratio of local to global worst-case SAR was calculated to evaluate which worst-case SAR is higher and thus considered for the overestimation in the Eichfelder VOP compression.

In addition, a reduced set of local SAR matrices was derived in which all local SAR matrices dominated by the whole-body SAR matrix were removed. For this, the difference between the global whole-body SAR matrix and each local SAR matrix ($Q_{wb} - Q_{l,i}$) was analyzed using the eigenvalues. If all eigenvalues are positive (matrix positive semidefinite), the local SAR matrix is completely dominated by the whole-body SAR matrix for all magnitude and phase combinations and can be removed from the set of local SAR matrices.² This process can be used as a pre-compression before the VOP compression.

3 | RESULTS

Figure 2 shows the distribution of local vs. whole-body SAR for 15 000 out of 1 million random shims. The plot axes were chosen to include the IEC SAR limits in normal and first-level operating mode. In all test cases, the local SAR limit was reached before the whole-body limit. From all random shims, the ratio local to whole-body SAR was found to be at least 9.2 for cases with the arms at the body sides (Figure 3). In this case, the local SAR limit was reached while the whole-body SAR reached up to

54% of the associated global limit. The 30-channel configuration with the arms above the head and thus outside the FOV of the RF antenna shows a smaller deviation between local and whole-body SAR, with local SAR being at least 8.5 times higher than whole-body SAR (58% of whole-body SAR when the local SAR limit was reached). The 24 and 30-channel arrays exhibit a lower minimum ratio of local to whole-body SAR. Figure 3 also shows the maximum ratio of local to whole-body SAR, which relates to the extent to which the local SAR is exceeded when only whole-body SAR is supervised. For the 2-channel birdcage,

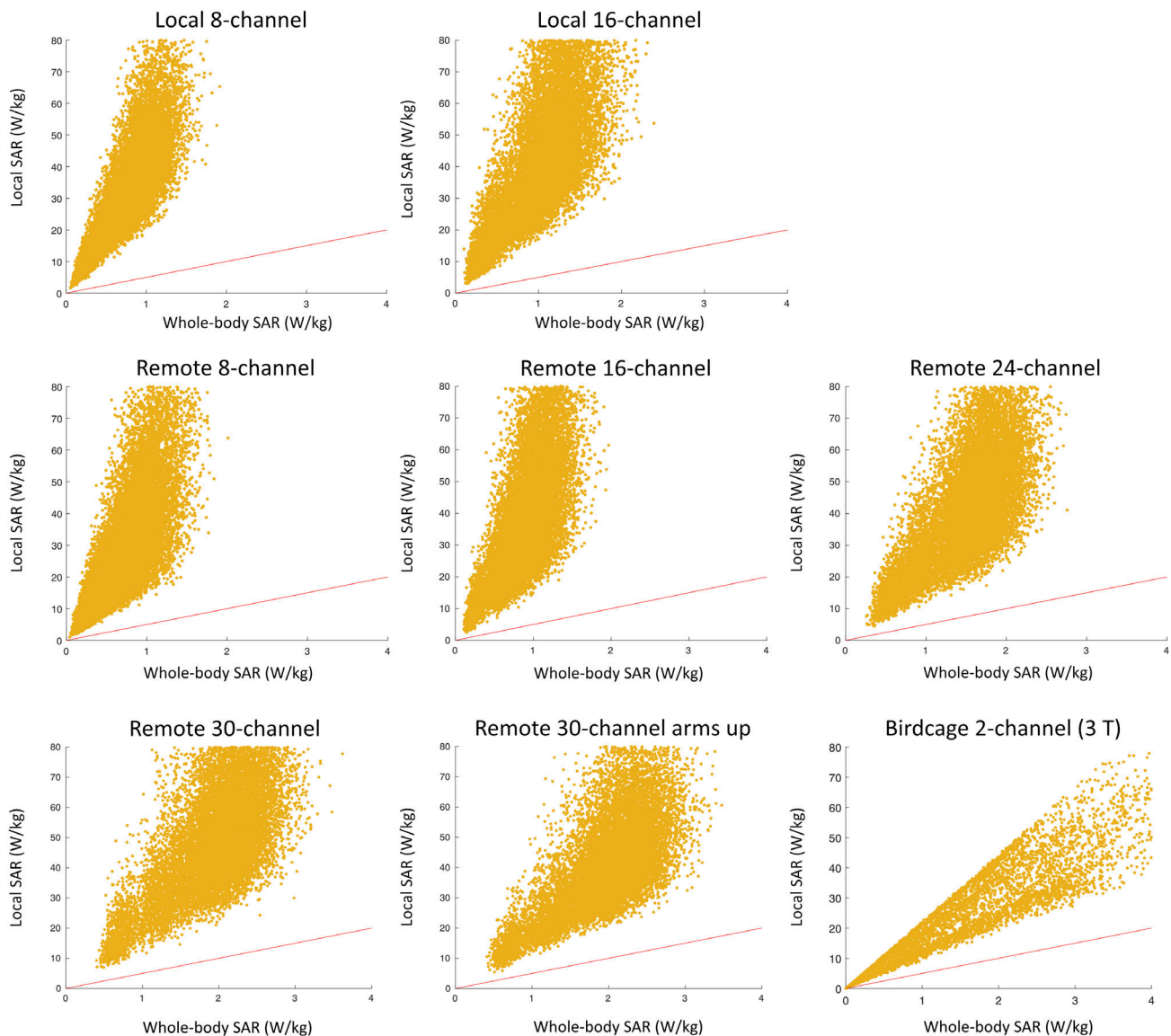


FIGURE 2 Maximum local versus whole-body SAR for 15 000 out of 1 million random shims. The red line indicates operating points where the IEC local and whole-body SAR constraints are equally restrictive; local SAR is more restrictive above this line. In all cases, the local SAR limit is reached before the whole-body SAR limit. For visual representation, the random shim vectors were grouped with amplitude u_{\max} and $u_{\max}/2$, which is most obvious in the plot for the 30-channel array. Although all configurations have results located close to the origin, with increasing number of channels the random choice of shims concentrates more points at higher SAR values away from the origin due to the increase in the degrees of freedom. Figure 3 shows the corresponding minimum ratio of local to whole-body SAR from all random shims.

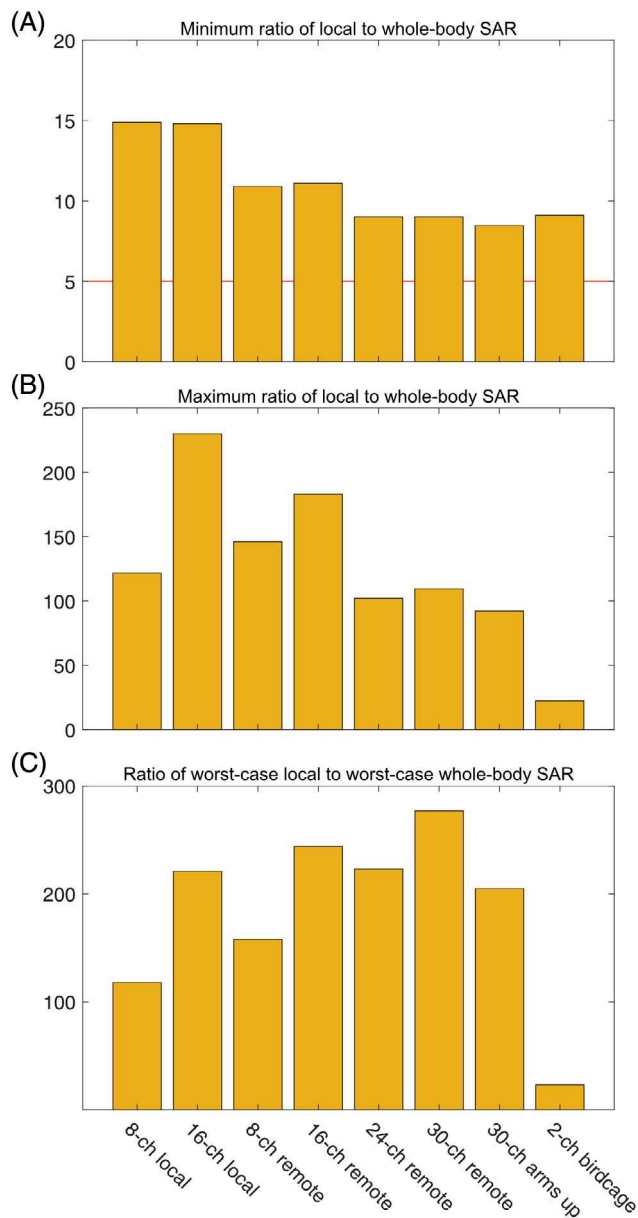


FIGURE 3 (A) Minimum and (B) maximum ratio of local to whole-body SAR from all random shims (see Figure 2). A ratio of 5 corresponds to a local SAR of 10 W/kg and whole-body SAR of 2 W/kg (SAR limits in normal operating mode, see Table 1). Values above 5 in (A) indicate that the local SAR limit is more restrictive. Values in (B) indicate the maximum local SAR that is induced when only whole-body SAR is supervised. (C) Ratio of worst-case local SAR to worst-case whole-body SAR. The worst-case local SAR is higher in all cases. The ratio for the two-channel 3 T birdcage coil is 23.

a local SAR of 44.4 W/kg was found when the whole-body SAR reached its limit of 2 W/kg.

The SAR matrices for the local 16-channel array were compressed to VOPs with different algorithms and overestimations, and the minimum, mean, and maximum value of the ratio maximum local vs. whole-body SAR

are shown in Table 1 (all other configurations are presented in Table S2). In addition, the table shows the results for the uncompressed set of SAR matrices and the respective number of matrices (uncompressed and compressed). The ratio of worst-case local SAR to worst-case whole-body SAR is shown in Figure 3C, always showing a higher worst-case local SAR for all antenna configurations, indicating that the local worst-case SAR will be used as overestimation during a VOP compression.

Regarding the reduction of the number of local SAR matrices by the whole-body SAR matrix, a reduction by 66.7% was found for the local eight-channel configuration (from 6 185 379 to 2 269 688 matrices; 2.1 to 0.8 GB). However, the reduction decreases for arrays with higher channel count to only 10.3% for the 30-channel array (6 950 090 to 6 235 648 matrices; 31.5 GB to 27.9 GB). The number of matrices for the 3 T birdcage was reduced by 87.9% (1 248 529 to 151 049; 22 MB to 3 MB). The results are summarized in Figure 4.

4 | DISCUSSION

Supervision of local SAR is critical in UHF MRI, as multi-channel transmit arrays in combination with the shorter RF wavelength can induce high local electric fields in the subject. However, with the development of antenna arrays with large FOV for body imaging, the question arises whether local or whole-body SAR is the most critical SAR aspect.

The results indicate that all considered RF transmit arrays for body imaging at 7 T in this study are constrained by the local SAR limit and that supervision based only on whole-body SAR would exceed the local SAR limits by several times. The deviation between whole-body and local SAR is nevertheless smaller for arrays with large FOV, as these arrays expose a larger part of the human body. Nevertheless, consideration of the (single) SAR matrix for the global SAR aspect increases the computational demand for safety supervisions only negligibly.

The 3 T birdcage also reached the local SAR limit before the whole-body SAR limit, with a similar ratio of local to whole-body SAR as found at 7 T. Similar values (ratios between 10 and 13) have been reported previously for a 3 T birdcage with two different body models.¹⁵ For a volume transmit coil such as the birdcage, however, supervision of the global SAR aspects is sufficient when partial body is selected instead of local SAR,⁶ which in turn indicates that potentially a high local SAR is induced when adhering to only global SAR limits. This result highlights a possible need for the additional mandatory supervision of local SAR for volume transmit coils, although the history of safe use indicates that the local SAR limits may instead need

TABLE 1 16-channel local array configuration: Minimum, mean, and maximum ratio of maximum local SAR (VOPs) versus whole-body SAR for 1 million random shims. VOP compression was performed with the algorithm by Eichfelder and Gebhard⁸ (10%, 5%, and 2.5% maximum overestimation of worst-case SAR) and with the hybrid algorithm by Orzada, Fiedler, and Ladd¹⁷ (1% and 0.25% overestimation of mean of all matrices normalized on the minimum real eigenvalue of all matrices). Whole-body SAR is defined with a single matrix. The evaluation with the uncompressed local SAR matrices is shown as reference. The memory requirement is given for single precision. Results for the other antenna arrays can be found in Table S2.

	No. of local SAR matrices	Ratio of maximum local to whole-body SAR		
		Minimum	Mean	Maximum
Eichfelder 10%	106	27.3	67.8	236.0
Eichfelder 5%	429	20.4	59.3	226.5
Eichfelder 2.5%	1771	17.8	55.5	236.0
Orzada 1%	365	15.6	56.2	225.8
Orzada 0.25%	1608	15.6	53.3	240.4
Uncompressed matrices: Full set / full set reduced by whole-body matrix (memory requirement)	9 626 832 / 3 756 513 (12.1 GB / 5.0 GB)	14.8	52.3	230.0

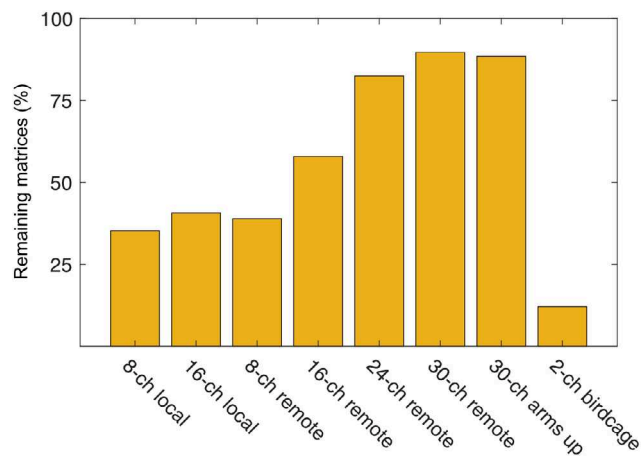


FIGURE 4 Reduction in the number of local SAR matrices by checking which are dominated by the whole-body SAR matrix. Of the arrays, the eight-channel configuration shows the highest reduction in local SAR matrices to 33.3% remaining matrices. The 3 T birdcage has only 12.1% remaining matrices.

adjustment. With the evaluation of the maximum ratio of local to whole-body SAR, we presented information about the highest local SAR levels during supervision based only on global SAR.

As shown previously, VOP compression algorithms increase calculated local SAR due to the incorporated overestimation. This overestimation is expected to be smaller in the future as VOP compression algorithms continue to improve^{16–18} and new supervision systems are developed to monitor a higher number of VOPs.¹⁹ Therefore, this study was performed with the uncompressed local SAR matrices, but results are also presented for compressions with different overestimation factors, which results in a

higher ratio of local to whole-body SAR, as global SAR aspects are represented with a single matrix and thus no compression is necessary.

The whole-body SAR matrix can be used to reduce the number of local SAR matrices, thus reducing the computational cost and hardware requirements for VOP compressions, enabling VOP compressions on workstations with less computing memory and saving hard disk memory. The step of reducing local SAR matrices and adding the whole-body SAR matrix to the set of matrices can be performed as a pre-compression prior to the conventional VOP compression. The reduction effect is particularly pronounced with the 8-channel arrays, which are currently the most used configuration for pTx imaging at 7 T and above, although these arrays are least constrained by the matrix size and thus computational cost. In contrast, there is a trend toward a higher number of remaining matrices for arrays with higher channel count, which is related to the increase in the degrees of freedom in the electric field. The large degrees of freedom enable a higher possible local SAR, resulting in more local SAR matrices not dominated by the global whole-body SAR matrix. This limits the reduction effect for arrays with a higher number of channels, which also require larger amounts of computing memory during the VOP compression due to the much higher matrix sizes, although a 10% reduction in memory is still relevant considering the large data sets. This effect is also prevalent in arrays with multiple rings, where a larger part of the human body is exposed, but the total number of elements is also increased. As worst-case local SAR is typically the metric reached first, adding the global SAR matrix to the set of matrices does not increase the overestimation in the Eichfelder VOP compression.

5 | CONCLUSIONS

PTx transmit antenna arrays with large FOV for body imaging expose a large part of the human body and raise questions regarding the most critical SAR aspect. For the antenna arrays used for body imaging at 7 T as well as for the 3 T birdcage, all evaluated cases show that the local SAR limit was reached before reaching the whole-body SAR limit, which highlights the relevance of local SAR supervision for pTx arrays and volume transmit coils.

Nevertheless, the study demonstrates that the whole-body SAR matrix can be included to reduce the number of local SAR matrices, which is important to reduce memory and computing time for a VOP compression. This step can be included as a pre-compression prior to the VOP compression.

ACKNOWLEDGEMENT

Open Access funding enabled and organized by Projekt DEAL.

ORCID

Thomas M. Fiedler  <https://orcid.org/0000-0002-1556-375X>

Stephan Orzada  <https://orcid.org/0000-0001-9784-4354>

REFERENCES

- Fiedler TM, Ladd ME, Bitz AK. SAR simulations & safety. *NeuroImage*. 2018;168:33-58. doi:10.1016/j.neuroimage.2017.03.035
- De Zanche N, van den Berg C, Brunner D, et al. ISMRM best practices for safety testing of experimental RF hardware. *International Society for Magnetic Resonance in Medicine (ISMRM)*. 2022;1-119. doi:10.7939/r3-7vpe-x737
- Zhu Y. Parallel excitation with an Array of transmit coils. *Magn Reson Med*. 2004;51:775-784. doi:10.1002/mrm.20011
- Deniz CM. Parallel transmission for ultrahigh field MRI. *Top Magn Reson Imaging*. 2019;28:159-171. doi:10.1097/RMR.0000000000000204
- Padormo F, Beqiri A, Hajnal JV, Malik SJ. Parallel transmission for ultrahigh-field imaging. *NMR Biomed*. 2015;29:1145-1161. doi:10.1002/nbm.3313
- IEC. 60601-2-33:2022 *Medical electrical equipment - Part 2-33: Particular requirements for the basic safety and essential performance, Edition 4.0: International Electrotechnical Commission (IEC)*.
- Uğurbil K, van de Moortele P-F, Grant A, et al. Progress in imaging the human torso at the ultrahigh fields of 7 and 10.5 T. *Magn Reson Imaging Clin N Am*. 2021;29:e1-e19. doi:10.1016/j.mric.2020.10.001
- Eichfelder G, Gebhardt M. Local specific absorption rate control for parallel transmission by virtual observation points. *Magn Reson Med*. 2011;66:1468-1476. doi:10.1002/mrm.22927
- Fiedler TM, Orzada S, Flöser M, et al. Performance analysis of integrated RF transmit antenna arrays with High Channel count for body imaging at 7 tesla. *NMR Biomed*. 2021;34:e4515. doi:10.1002/nbm.4515
- Fiedler TM, Orzada S, Flöser M, et al. Performance and safety assessment of an integrated transmit array for body imaging at 7 T under consideration of specific absorption rate, tissue temperature, and thermal dose. *NMR Biomed*. 2022;35:e4656. doi:10.1002/nbm.4656
- Stelter JK, Ladd ME, Fiedler TM. Numerical comparison of local transceiver arrays of fractionated dipoles and microstrip antennas for body imaging at 7 T. *NMR Biomed*. 2022;35:e4722. doi:10.1002/nbm.4722
- Adriany G, van de Moortele P-F, Wiesinger F, et al. Transmit and receive transmission line arrays for 7 tesla parallel imaging. *Magn Reson Med*. 2005;53:434-445. doi:10.1002/mrm.20321
- Christ A, Kainz W, Hahn EG, et al. The Virtual Family-development of surface-based anatomical models of two adults and two children for dosimetric simulations. *Phys Med Biol*. 2010;55:N23-N38. doi:10.1088/0031-9155/55/2/N01
- Graesslin I, Homann H, Biederer S, et al. A specific absorption rate prediction concept for parallel transmission MR. *Magn Reson Med*. 2012;68:1664-1674. doi:10.1002/mrm.24138
- Collins CM, Mao W, Liu W, Smith MB. Calculated local and average SAR in comparison with regulatory limits. *Proc Intl Soc Mag Reson Med*. 2006:2044.
- Orzada S, Fiedler TM, Bitz AK, Ladd ME, Quick HH. Local SAR compression with overestimation control to reduce maximum relative SAR overestimation and improve multi-channel RF array performance. *Magma*. 2020;34:153-163. doi:10.1007/s10334-020-00890-0
- Orzada S, Fiedler TM, Ladd ME. Hybrid algorithms for SAR matrix compression and the impact of post-processing on SAR calculation complexity. *Magn Reson Med*. 2024;92:2696-2706. doi:10.1002/mrm.30235
- Lee J, Gebhardt M, Wald LL, Adalsteinsson E. Local SAR in parallel transmission pulse design. *Magn Reson Med*. 2012;67:1566-1578. doi:10.1002/mrm.23140
- Fiedler TM, Grimm JA, Klein C, et al. Real-time SAR supervision for a 32-channel RF transmit system with virtual observation points. *Proc Intl Soc Mag Reson Med*. 2024;3747.

SUPPORTING INFORMATION

Additional supporting information may be found in the online version of the article at the publisher's website.

Table S1. Limits for global SAR aspects and localized SAR (adapted from IEC 60601-2-33:2022). Local RF transmit coils are controlled by local SAR and whole-body SAR; volume RF transmit coils by whole body SAR, head SAR and at least one of the following: partial body SAR or local SAR. SAR aspects are given for an averaging time of 6 min. *Determination of partial body SAR according to IEC 60601-2-33:2022.⁶

Table S2. In addition to Table 1, this supporting information lists the data for all evaluated antenna arrays. Minimum, mean, and maximum ratio of maximum local SAR (VOPs) vs. whole-body SAR for 1 million random shims. VOP compression was performed with the algorithm by Eichfelder and Gebhardt⁸ (10%, 5%, and 2.5% maximum overestimation of worst-case SAR) and with the hybrid

algorithm by Orzada, Fiedler, and Ladd¹⁷ (1% and 0.25% overestimation of mean of all matrices normalized on the minimum real eigenvalue of all matrices). Whole-body SAR is defined with a single matrix. The evaluation with the uncompressed local SAR matrices is shown as reference. The memory requirement is given for single precision.

How to cite this article: Fiedler TM, Ladd ME, Orzada S. Local and whole-body SAR in UHF body imaging: Implications for SAR matrix compression. *Magn Reson Med*. 2025;93:842-849. doi: 10.1002/mrm.30306